Pol. J. Environ. Stud. Vol. XX, No. X (XXXX), 1-15
DOI: 10.15244/pjoes/192373 ONLINE PUBLICATION DATE:

Original Research

Spatiotemporal Pattern and Influencing Factors of Carbon Dioxide Emissions at Prefecture Level Cities in China: 2000-2020

Rongwei Wu[1,2,3], Jiali Zhang[1], Yue Qi[1], Liang Zhou[2*]

[1]School of Public Administration, Chongqing Technology and Business University, Chongqing, 400067, China
[2]Faculty of Geomatics, Lanzhou Jiaotong University, Lanzhou 730070, China
[3]Population Development and Policy Research Center, Chongqing Technology and Business University, Chongqing, 400067, China

Received: 19 May 2024
Accepted: 15 August 2024

Abstract

Global warming caused by greenhouse gas emissions poses a significant challenge to the sustainable development of ecosystems and human society. It is crucial to conduct a comprehensive analysis of spatiotemporal dynamics and the underlying factors influencing CO_2 emissions at a finer spatial scale to advance strategies for mitigating CO_2 emissions. This study integrates energy consumption data, population grid data, and nighttime light data from 2000 to 2020 to construct a comprehensive evaluation system for estimating CO_2 emissions of prefecture-level cities (hereinafter referred to as cities) in China. On this basis, we introduced the Exploratory Spatial-Temporal Data Analysis (ESTDA) method to systematically reveal the spatiotemporal patterns of per capita CO_2 emissions in Chinese cities. Finally, an improved STIRPAT model is employed to analyze the influencing factors of per capita CO_2 emissions. A panel regression model is adopted to examine the relationship between per capita CO_2 emissions and population, urbanization, industrial structure, fixed investment assets, and total import and export volume with the panel data of 284 prefecture-level cities in China spanning from 2005 to 2020. The results indicate that:

1. There are huge regional differences in per capita CO_2 emissions among Chinese cities. Notably, northern cities generally exhibit higher per capita CO_2 emissions compared to southern cities. Moreover, certain provincial capital cities and independent plan cities display higher per capita CO_2 emissions than their surrounding cities.

2. From 2000 to 2020, the spatiotemporal dynamics of per capita CO_2 emissions in various cities demonstrated overall stability with localized variations. This stability is evidenced by the 85% spatiotemporal cohesion rate of per capita CO_2 emissions from 2000 to 2020, indicating a dominant status of no correlation pattern shift. Local dynamics are reflected in the fact that the spatial correlation structure of per capita CO_2 emissions in resource-based cities and some economically developed regions

*e-mail: zhouliang@lzjtu.edu.cn

has changed. From the three subtypes of spatiotemporal transitions, Type 1 (0.095)>Type 3 (0.074)>Type 2 (0.060), indicating that some resource-based cities have embarked on a low-carbon transformation development trend in China.

3. The panel data regression results reveal an inverted U-shaped relationship between economic growth and per capita CO_2 emissions at the prefecture-level city scale. Initially, per capita CO_2 emissions increase with economic growth, first increasing and then decreasing. Per capita CO_2 emissions are positively correlated with population size, the proportion of the secondary industry's value added to GDP, the proportion of fixed investment assets to GDP, and the proportion of total import and export value in GDP. Conversely, per capita CO_2 emissions. are negatively correlated with urbanization level and the proportion of the tertiary industry's value added to GDP.

Keywords: CO_2 emission, prefecture level cities, ESTDA, China

Introduction

Global climate change profoundly impacts human development and public health, presenting a substantial environmental challenge for the international community. The Sixth Assessment Report [1] states unequivocally that human activities have led to global warming, with the global average surface temperature increasing by 1.1°C between 2011 and 2020 compared with temperatures during the pre-industrial period (1850–1900). The primary sources of global greenhouse gas emissions are the energy and industrial sectors. The rapid pace of economic development has intensified energy consumption and environmental pressures, leading to a continuous rise in CO_2 emissions. This situation creates a dilemma where economic growth coincides with increased CO_2 emissions. Decoupling CO_2 emissions from economic growth is crucial for sustainable development and a critical issue that all nations must confront. Consequently, extensive attention has been devoted to researching the spatiotemporal dynamics of CO_2 emissions and their influencing factors. An analysis of CO_2 spatiotemporal variations from 1990 to 2016 at global, regional, and national scales found that China had the highest annual CO_2 growth rate and industrial emissions worldwide. Statistics from the International Energy Agency (IEA) [2] indicate that China has been the world's largest CO_2 emitter since 2007, with CO_2 emissions exceeding 12.1 billion tons in 2022, accounting for approximately 33% of the global total. To promote sustainable development, at the United Nations Climate Conference in September 2020, the Chinese government unveiled targets to peak carbon emissions by 2030 and achieve carbon neutrality by 2060. This pledge marks a pivotal shift from focusing on "relative emissions decreases" to pursuing "absolute emissions reductions", The strategy aims to decouple socioeconomic growth from carbon emissions, ensuring a greener path forward for national prosperity.

To better understand the spatiotemporal dynamics and determinants of CO_2 emissions in China, scholars have extensively examined CO_2 emissions characteristics across its provinces and cities, focusing on total CO_2 emissions, per capita CO_2 emissions, and CO_2 emission intensity. These studies have consistently shown a rising trend in both total and per capita CO_2 emissions, with high-emission areas clustering along the coastal and northern regions of the country [3]. Moreover, the geographic center of CO_2 emissions has shifted from the eastern to the western regions [4]. Factors such as energy intensity, industrial structure, urbanization level, the proportion of fixed investment assets in GDP, and the ratio of total import and export value to GDP have significant impacts on CO_2 emissions [5]. Due to China's distinctive political and administrative system, fulfilling the national CO_2 abatement goals depends on cascading these objectives through different administrative levels, with cities being the primary agents for achieving these reductions [6]. Nonetheless, the National Bureau of Statistics of China only publishes energy consumption data for 30 provincial-level administrative regions, which obstructs the revelation of CO_2 emissions and their causes at the city level. Consequently, downscaling the estimation of CO_2 emissions becomes crucial for addressing this issue.

To tackle the problem of downscaling CO_2 emission estimates, Ghosh et al. [7] pioneered the method of correlating nighttime light data with CO_2 emissions to model emissions at a finer geographical resolution. Subsequent scholars expand on this approach. For instance, Wang and Ye [8] utilized single-year nighttime light data to estimate city level CO_2 emissions throughout China in 2013, highlighting the positive correlation between CO_2 emissions and economic growth. Wang and Liu [9] employed multi-period nighttime light data to reveal an inverted U-shaped relationship between per capita CO_2 emissions and economic development at the city level from 1992 to 2013. With the emergence of the new generation of nighttime light data, NPP-VIIRS, researchers have attempted to integrate DMSP/OLS nighttime light data with NPP-VIIRS satellite data for long-term sequence analysis. Chen et al. [10] created an extended time series of NPP-VIIRS nighttime light data from 2000 to 2018 by combining the DMSP-OLS nighttime light data from 2000 to 2012, which was calibrated with a new cross-sensor, and monthly NPP-VIIRS nighttime light data from 2013 to 2018. They also estimated CO_2 emissions for 2,735 counties in China

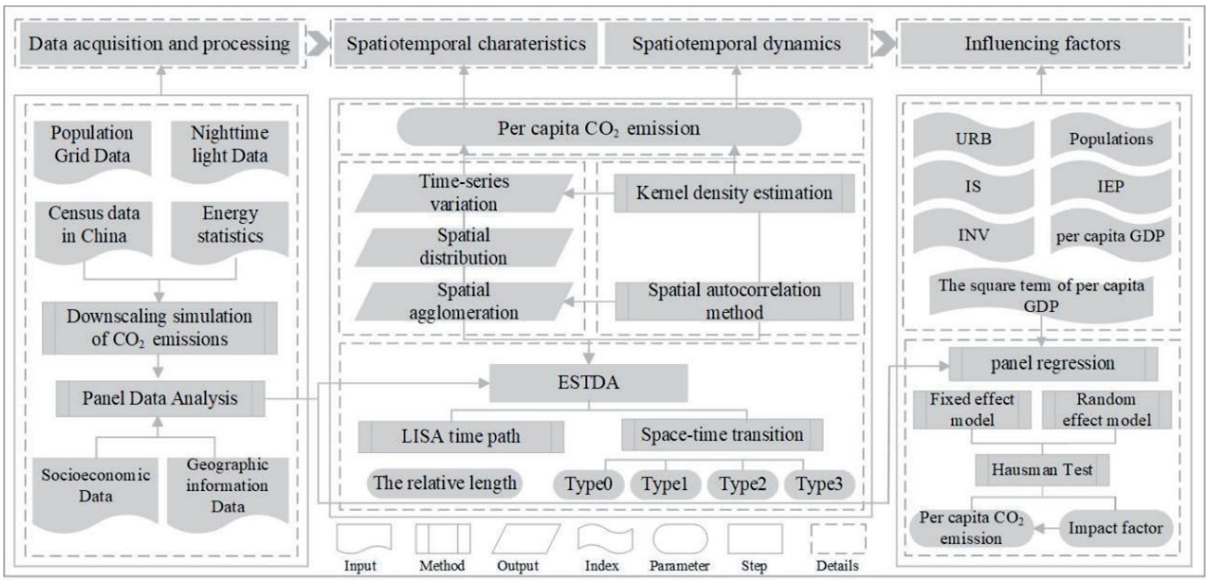

Fig. 1. Schematic of research framework.

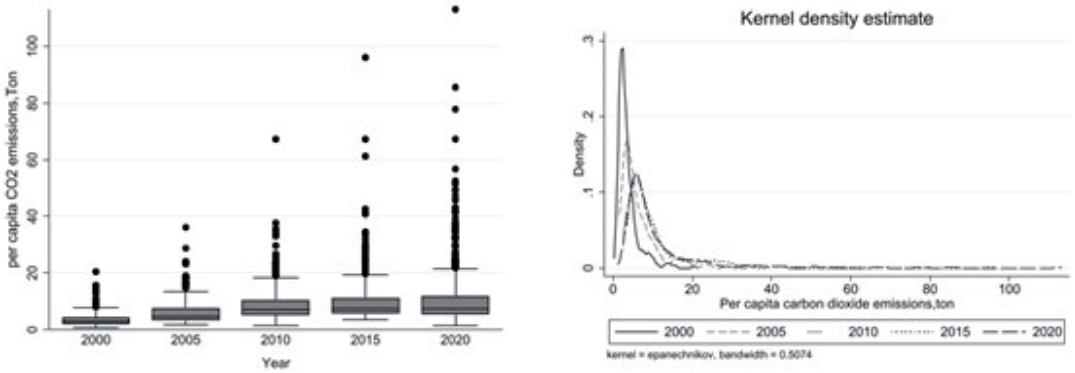

Fig. 2. Box plot of per capita CO_2 emissions in Chinese cities and kernel density estimation curve of per capita CO_2 emissions in Chinese cities.

from 1997 to 2017 using the PSO-BP algorithm, unifying the scales of DMSP-OLS and NPP-VIIRS satellite images [11]. While earlier studies relied on nighttime light data alone to estimate CO_2 emissions at smaller administrative scales, recent research indicates that incorporating nighttime light with population grid data yields better estimation accuracy. For example, Ou et al. [12] combined population grid data with nighttime light data to more accurately estimate China's CO_2 emissions in 2012. Building upon this foundation, Chen et al. [13] used corrected nighttime light data and population data to estimate CO_2 emissions for Chinese cities in 2015, validating results against energy consumption data, and demonstrating the feasibility of this estimation method for studying China's CO_2 emissions.

In addition, Grossman and Krueger [14] introduced the Environmental Kuznets Curve (EKC) hypothesis to examine the relationship between environmental degradation and income levels. Subsequent scholars across various countries and regions have utilized diverse econometric methodologies to explore the association between CO_2 emissions and the EKC premise. These investigations have revealed a spectrum of EKC relationships, including U-shaped, inverted U-shaped, and N-shaped curves. For instance, research on CO_2 emissions and economic growth in Chinese provinces has confirmed an inverted U-shaped EKC [9, 13], allowing for an accurate assessment of the curve's form and inflection points. Additionally, several prominent academics have identified an N-shaped relationship between economic development and environmental pollution in China [15]. However, some argue that the EKC hypothesis does not adequately apply to China. Pata and Caglar [16] used the Augmented Autoregressive Distributed Lag model to investigate annual time series data from 1980 to 2016 and found a U-shaped quadratic relationship between environmental pollution and income levels.

To sum up, this article improves existing research from the following aspects: Firstly, it utilizes an

extensive time-series dataset of nighttime light data spanning from 2000 to 2022, established by Wu et al. [17]. Building upon this foundation, we implement the methodology proposed by Chen et al. [10], integrating population grid data and nighttime light data to estimate CO_2 emissions for cities in China, while subsequently, employing ESTDA to uncover the spatiotemporal dynamics of per capita CO_2 emissions at the city scale. Finally, using an expanded STIRPAT model and panel data regression, we identify the factors influencing the dynamic evolution of CO_2 emissions.

The marginal contribution of this article lies in proposing a method for estimating CO_2 emissions at the prefecture level city scale and applying this method to estimate the CO_2 emissions of Chinese cities from 2000 to 2020. In addition, we apply panel data regression to investigate the presence of an environmental Kuznets curve between economic growth and CO_2 emissions at this scale.

Material and Methods

The empirical research framework of this paper is shown in Fig. 1. It commences with the use of energy consumption data, population grid data, and nighttime light data to estimate CO_2 emissions at the city scale. Subsequently, kernel density estimation is used to reveal the evolutionary characteristics of CO_2 emissions, including changes in distribution location, distribution form, distribution expansion, and polarization trend [18]. Concurrently, the ESTDA method is employed to comprehensively analyze the spatiotemporal dynamics of CO_2 emissions across Chinese cities. Finally, a panel data regression model is used to identify the factors influencing CO_2 emissions at the city scale.

Data Sources

This study relies on several main data sources: 1. Population data: population density data (2000-2020) is obtained from the Global High-Resolution Population Project (https://landscan.ornl.gov/), along with census data and a 1% population sample survey data from the National Bureau of Statistics. 2. Nighttime light data was integrated by Wu et al. [17] using the "pseudo-invariant pixel" method from DMSP-OLS and SNPP-VIIRS and is available at https://dataverse.harvard.edu/dataset.xhtml?persistentId=doi:10.7910/DVN/GIYGJU. This dataset spans from 1992 to 2022, ensuring comparability and consistency across different satellite sensors. The data were projected into the Albers equal-area projection and resampled to a resolution of 1km×1km for this study. 3. Energy consumption data is primarily sourced from the "China Energy Statistical Yearbook", spanning from 2001 to 2021, while carbon emission coefficients are derived from the "2006 IPCC Guidelines for National Greenhouse Gas Inventories." 4. Socioeconomic data is obtained from the "China City Statistical Yearbook" spanning from 2001 to 2021.[1]

Fitting Prefecture-Level City-Scale CO_2 Based on Nighttime Lighting and Population Data

Measuring CO_2 Emissions from Provincial Energy Consumption

Building upon the CO_2 emissions calculation methodology proposed by the IPCC, this study focuses on eight primary energy sources—coal, coke, crude oil, gasoline, kerosene, diesel, fuel oil, and natural gas—to estimate CO_2 emissions. The calculation Equation is as follows [19]:

$$TCO_2 = \sum_{i=1}^{8} (CO_2)^i = \sum_{i=1}^{8} E_i \times NCV_i \times CEF_i \quad (1)$$

Where: E_i represents the total CO_2 emissions, while NCV_i refers to the average low-order calorific value of each type of fossil energy, obtainable from Appendix 4 of the China Energy Statistical Yearbook 2011. Additionally, CEF_i denotes the CO_2 emission coefficients of the i^{th} energy provided by the IPCC.

Estimation of CO_2 Emissions

The estimation method used was proposed by Elvidge et al. [20] and Chen et al. [13]. This method is a top-down process that allocates large-scale CO_2 emission data to finer grid units based on a combination of nighttime lighting and population grids. For the light areas, CO_2 emissions are proportional to the lighting values, but in such areas, the population data is an effective proxy for detecting CO_2 emissions, and thus, the population raster data is used to measure CO_2 emissions in the light areas. Referring to the studies of Ou et al. [12] and Chen et al. [13], the per capita CO_2 emissions of dark areas are half that of light areas, thus it can be assumed that the CO_2 emissions of light areas and dark areas of each province j are X_j and $1/2\ X_j$, respectively. Based on the above, the detailed calculation process is as follows:

(1) Population raster data calibration:

The national population census and the national 1% population sample survey are the most authoritative sources of population data published by the Chinese

1 Around the year 2000, China was experiencing a period of frequent changes in the delineation of its prefectural-level administrative divisions, leading to substantial variations in the number of cities. These changes were largely completed by 2005. The redrawing of administrative boundaries between 2000 and 2005 has resulted in poor comparability of data among cities during this period. To mitigate the impact of these changes on the comparability of statistical data, this study focuses on the period from 2005 to 2020 for the analysis of factors influencing CO_2 emissions.

government. The population data for Chinese cities are obtained from the yearbooks of the previous population censuses and the 1% population sample surveys, and the population raster data are calibrated after resampling. The basic logic of the calibration is to summarize the population of each city in the spatial scope based on the population raster data, compare the obtained population with the real population obtained from the population census, and obtain the calibration coefficients. Subsequently, the population raster data for each city is multiplied by the corresponding calibration coefficient.

(2) Measuring CO_2 emissions:

1. Provincial-scale CO_2 emissions are calculated as follows: The provincial nighttime lighting data is overlaid with the population raster data for analysis, using the nighttime lighting data as a mask. The population raster data is extracted to obtain the population data from the light areas of each administrative unit $j(SP_{Lj})$ and the population data of the dark areas of each administrative unit $j(SP_{Dj})$ The total CO_2 emissions of light and dark areas in administrative unit j (CO_{2Lj}, CO_{2Dj}) are calculated using:

$$CO_{2Lj} = SP_{Lj} * X_j \tag{2}$$

$$CO_{2Dj} = SP_{Dj} * \frac{1}{2} X_j \tag{3}$$

In Equations (2) and (3), the provincial per capita CO_2 emissions are:

$$X_j = TCO_{2j} / (SP_{Lj} + SP_{Dj} / 2) \tag{4}$$

The carbon emissions in light and dark areas constitute the total CO_2 emissions of administrative unit $j(TCO_{2j})$, as follows:

$$TCO_{2j} = CO_{2Lj} + CO_{2Dj} \tag{5}$$

2. This is calculated as being equal to the ratio of the total CO_2 emissions of light areas of administrative unit $j(CO_{2Lj})$ and the total light value of administrative unit $j(T_{Lj})$. Then, each light grid's radiation value in administrative unit $j(L_{gj})$ is multiplied by the ratio described above. Thus, the light areas' CO_2 emissions grid value of the administrative unit $j(CO_{2Lgj})$ is acquired by:

$$CO_{2Lgj} = L_{gj} * (CO_{2Lj} / T_{Lj}) \tag{6}$$

Similarly, for city dark areas, CO_2 emissions per capita are equal to the ratio of total CO_2 emissions to total population in the provincial dark areas. Therefore, the total CO_2 emissions of the dark-value area are equal to the product of the CO_2 emissions per capita and the population of the dark-value area (P_{Dgj}). The calculation formula is as follows:

$$CO_{2Dgj} = P_{Dgj} * (CO_{2Dj} / SP_{Dj}) \tag{7}$$

According to Equations (5) and (6), the total CO_2 emissions of administrative unit j are equal to the sum of CO_2 emissions from light areas (CO_{2Lgj}) and CO_2 emissions from dark areas (CO_{2Dgj}) in administrative unit j of all the corresponding cities, where

$$CO_{2j} = \sum_{g=1}^{N} CO_{2Lgj} + \sum_{g=1}^{M} CO_{2Dgj} \tag{8}$$

Exploratory Spatiotemporal Data Analysis Methods

The ESTDA analytical framework proposed by Rey and Janikas [21] effectively extends the ESDA method in terms of time dimension and realizes the benign coupling of temporal-spatial measures, which mainly includes analysis techniques such as Local Indicators of Spatial Association (LISA), LISA time path, and LISA spatiotemporal transition. ESTDA was further introduced to reveal the spatiotemporal structural characteristics of per capita CO_2 emissions at the city scale in China.

LISA Time Path

The LISA time path is a continuous expression of the positional shift of spatial units in the Moran scatterplot and a continuous expression of the LISA Markov shift matrix. By visualizing the pairwise shifts of an attribute value of a spatial cell with its neighborhood mean (spatial lag), revealing the extent and direction of the spatiotemporal interactions of per capita CO_2 emissions between regions, it further reveals how spatiotemporal dependence shapes the developmental trajectory of the regional system. In this paper, we utilize the LISA time path metrics for the per capita CO_2 emissions of each city. The leapfrog path of city i in Moran's I scatterplot can be regarded as a set of vectors $[(y_{i,1},yl_{i,1}),(y_{i,2},yl_{i,2}),\cdots,(y_{i,T},yl_{i,T})]$, where $y_{i,t}$ is the per capita CO_2 emission of city i in year t, and $yl_{i,t}$ is its spatial lag of per capita CO_2 emissions in year t [22]. The LISA temporal path length is expressed as:

$$d = \frac{N \sum_{t=1}^{T-1} d(L_{i,t}, L_{i,t+1})}{\sum_{i=1}^{N} \sum_{t=1}^{T-1} d(L_{i,t}, L_{i,t+1})} \tag{9}$$

Where: N denotes the number of cities; T is the annual time interval; $L_{i,t}$ represents the LISA coordinates of the city in year t; $d(L_{i,t},L_{i,t+1})$ is the moving distance of city i from year t to year $t+1$. The larger the d, the stronger the dynamics of the local spatial structure; $d>1$ means that the moving distance of the city is larger than the average value of the moving distance of the city.

LISA Spatiotemporal Transition

LISA provides a local perspective to reveal spatial dependencies between study units [23]. Ye and Rey [24] proposed the concept of spatiotemporal transition based on the shifting of the types of local spatial associations of the units in Moran's I scatterplot at different time periods. The spatiotemporal transition is classified into four types: Type0, Type1, Type2, and Type3 [25]. Among them, Type0 indicates that both city and its neighborhood do not undergo spatiotemporal transitions, all of which are located on the main diagonal of the transfer matrix; Type1 indicates that the city itself transitions while its neighborhood remains stable, including $HH_t \rightarrow LH_{t+1}$, $HL_t \rightarrow LL_{t+1}$, $LH_t \rightarrow HH_{t+1}$, $LL_t \rightarrow HL_{t+1}$; Type2 indicates that the city itself remains unchanged, but its neighborhood transition includes $HH_t \rightarrow HL_{t+1}$, $HL_t \rightarrow HH_{t+1}$, $LH_t \rightarrow LL_{t+1}$, $LL_t \rightarrow LH_{t+1}$; Type3 indicates that both the city itself and the neighborhood leap, and this type can be further divided into Type3A and Type3B, the former indicating that the city itself and the neighborhood have the same direction of the transition, including $HH_t \rightarrow LL_{t+1}$, $LL_t \rightarrow HH_{t+1}$; the latter indicates that the directions of the two transitions are opposite, and includes $HL_t \rightarrow LH_{t+1}$, $LH_t \rightarrow HL_{t+1}$. For spatiotemporal variability and coalescence in a regional system, Rey and Ye [22] define it as during this study period the ratio of the number of transitions of a certain type to the total number of transitions (m) that may be present in the system, m=336.

The spatiotemporal variation is expressed as

$$SF = \frac{F_1 + F_2}{m} \tag{10}$$

The spatiotemporal cohesion Equation is

$$SC = \frac{F_0 + F_{3A}}{m} \tag{11}$$

Where: F_0, F_1, F_2, and F_{3A} denote the number of leaps for Type0, Type1, Type2, and Type3A, respectively.

Analysis of Factors Influencing CO_2 Emissions Based on the STIRPAT Model

Based on IPAT and ImPACT, York et al. [26] proposed the STIRPAT model. The model is widely used as it makes it possible to decompose the factors in the model or extend the model by incorporating other influencing factors according to the needs of practical applications. The base form of the model is:

$$I_i = \alpha P_i^b A_i^c T_i^d e_i \tag{12}$$

Where: α is the model coefficient; I denotes the environmental pressure; P, A, and T are the population factor, affluence factor, and technology factor, respectively; b, c, and d are the indices of the population factor, the influence factor, and the technology factor, and e represents the disturbance term. The linear regression equation can be obtained by logarithmic treatment of both sides of Equation (12):

$$\ln I_{it} = \alpha + b(\ln P_{it}) + c(\ln A_{it}) + d(\ln T_{it}) + e_{it} \tag{13}$$

Where: i denotes individuals; t represents year; b, c, and d are indices of P, A, and T, respectively; e is a disturbance term; and α is a constant. Equation presents a linear relationship between population, affluence, and technology.

This study extends the model with the following explanations: Existing research has analyzed the relationship between economic factors and CO_2 emissions, with the Environmental Kuznets Curve (EKC) hypothesis serving as a classic analytical paradigm. This hypothesis posits a nonlinear relationship between per capita income and per capita CO_2 emissions. To test the EKC hypothesis, our study incorporates per capita GDP (PCGDP) and its quadratic term (PCGDP_sq) as key factors [27], capturing the impact of economic development on the environment.

Urbanization represents a dynamic process characterized by the concentration of population in urban areas, promoting urban development and significantly transforming social, economic, and production structures, as well as lifestyle, while urbanization can improve energy efficiency and reduce CO_2 emissions [28]. It concurrently drives up energy demand due to population aggregation [29]. This increased demand fuels the construction of urban infrastructure and the demand for energy-intensive, polluting products, thereby further escalating CO_2 emissions [30]. Therefore, the urbanization rate, represented by the ratio of urban permanent residents to the total urban population (denoted as URB), emerges as a critical factor influencing CO_2 emissions.

Population size (denoted as POP) has consistently been shown in previous research to be positively correlated with CO_2 emissions [5, 31]. Population growth increases energy consumption, subsequently driving up CO_2 emissions.

Economic growth is intricately related to various industrial sectors, with alterations in the industrial structure significantly impacting CO_2 emissions [32]. The secondary industry, encompassing carbon-intensive sectors such as manufacturing and construction, exerts a substantial influence on CO_2 emissions compared to agriculture and the tertiary industry. This study incorporates the proportion of secondary industry value added to GDP (SIP) and the proportion of tertiary industry value added to GDP (TIP) to measure the industrial structure.

Fixed-asset investment as a proportion of GDP (denoted as INV) is crucial, as increased investment drives substantial fossil energy consumption, thereby intensifying CO_2 emission intensity [33]. Domestic investment-generated CO_2 emissions constitute

approximately one-third of China's total CO_2 emissions, primarily from the construction and manufacturing sectors. Therefore, the proportion of fixed-asset investment to GDP serves as a proxy variable for CO_2 emissions [34].

The proportion of total imports and exports to GDP (denoted as IEP) serves as an indicator of trade intensity. The impact of trade openness on China's CO_2 emissions is widely debated, with both positive and negative effects of imports and exports on CO_2 emissions [30]. Higher trade openness can lead to increased exports of energy-intensive products, thereby increasing pollution. With exports constituting approximately one-third of China's GDP [35], CO_2 emissions are influenced not only by domestic consumption but also by long-term trends in foreign trade, which could potentially reduce CO_2 emissions. However, in the short term, foreign trade tends to have a negative impact on CO_2 emissions [35].

Combining the above sections, the STIRPAT model was extended to analyze the influencing factors of city CO_2 emissions using a panel regression model and constructing the following Equations:

$$\begin{aligned} \ln PCCE_{it} &= \alpha + b(\ln PCGDP_{it}) \\ &+ c(\ln PCGDP\_sq_{it}) + d(\ln URB_{it}) \\ &+ f(\ln POP_{it}) + g(TIP_{it}) + h(SIP_{it}) \\ &+ j(INV_{it}) + k(IEP_{it}) + e_{it} \end{aligned} \quad (14)$$

Where: i and t represent the observation sample and time, respectively. *PCCE* indicates per capita CO_2 emissions; *PCGDP* stands for per capita GDP value; *URB* stands for urbanization rate; *POP* refers to population size, *SIP* stands for the share of value added in the secondary industry in GDP, *TIP* represents the share of value added in the tertiary industry in GDP *INV* signifies the share of fixed investment assets in GDP, and *IEP* stands for the share of total imports and exports in GDP. α denotes the constant term; e stands for the unobservable interference term; and b-d and f-g represent the correlation coefficients of each influencing factor individually.

Results

Temporal Trends in City per Capita CO_2 Emissions

As illustrated in Fig. 3, China's per capita CO_2 emissions in cities exhibit a trend of fluctuating increase from 2000 to 2020. In 2000, per capita CO_2 emissions mainly ranged from 1.9 to 4.3 tons; by 2010, this range had increased to 4.9 to 11 tons, and by 2020, it had further expanded to 5.5 to 13 tons. From 2000 to 2020, both the minimum and maximum per capita CO_2 emissions in Chinese cities have increased, reflecting a more volatile and imbalanced distribution compared to the periods of 2000 and 2010.

In terms of concentration, the per capita CO_2 emissions in Chinese cities were more centralized in the early years. After 2010, the box plots show longer lengths, indicating a more dispersed distribution. The kernel density plots of per capita CO_2 emissions in Chinese cities over five years reveal that the trend in the distribution's skewness remains relatively constant. However, the kernel density curve has widened and slightly shifted to the right, with a decrease in peak values. These findings suggest a gradual increase in per capita CO_2 emissions in Chinese cities and reflect the growing regional disparities from 2000 to 2020. Related studies [16, 36] have demonstrated that economic growth, urbanization, and other factors exhibit a non-linear relationship with per capita CO_2 emissions. With the increase of economic development or urbanization, per capita CO_2 shows a trend of first increasing and then decreasing. Different cities are at different stages, resulting in an increasing variability and gap in per capita CO_2 emissions between cities.

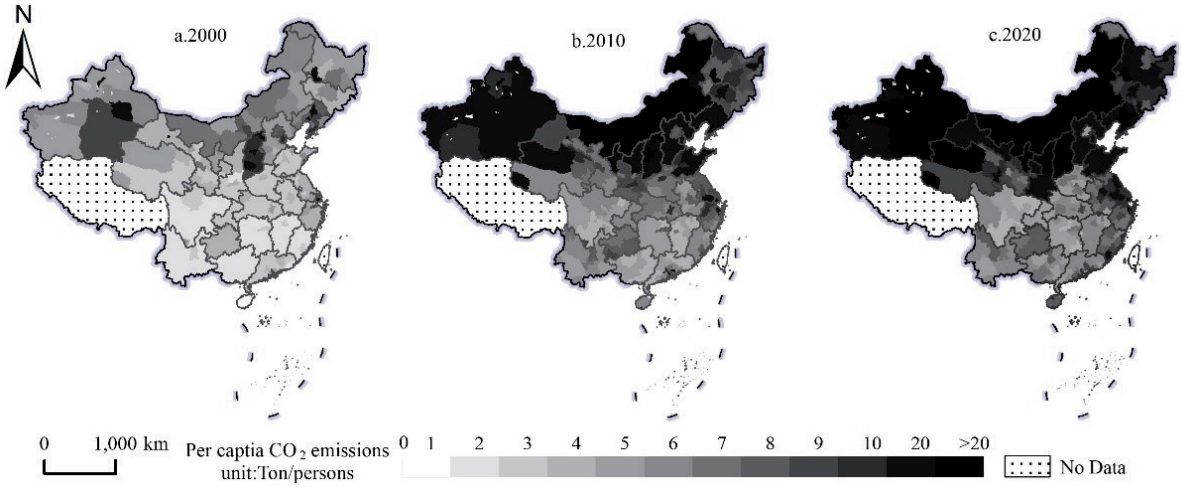

Fig. 3. The spatiotemporal evolution of per capita CO_2 emissions at the city scale in China.

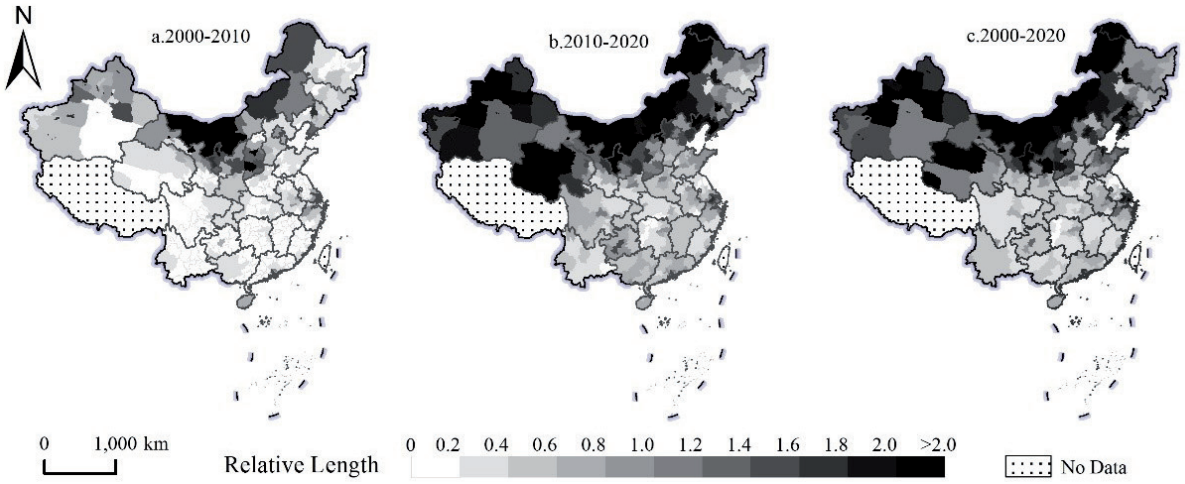

Fig. 4. The relative length of time paths for per capita CO_2 emissions at different stages at city scale in China.

Overall Distribution Pattern of City CO_2 Per Capita

Based on the per capita CO_2 emissions data, the natural breakpoint method of classification is utilized to draw the spatial distribution of per capita CO_2 emissions in Chinese cities in 2000, 2010, and 2020, which can be seen in Fig. 3.

Per Capita CO_2 Emissions Are Generally Higher in Northern Cities Than in Southern Cities.

The per capita CO_2 emissions in northern cities are generally higher than those in southern cities, reflecting a distribution pattern where emissions are more prevalent in the north. This disparity is primarily attributed to two factors: Firstly, the northern regions of China possess abundant fossil energy resources such as coal, oil, and natural gas. Cities like Yulin in Shaanxi Province; Datong, Yangquan, and Linfen in Shanxi Province; and Erdos City, Huolingol, and Alxa League in Inner Mongolia highly rely on these resources for socio-economic development, leading to the formation of industry clusters characterized by high energy consumption and emissions. Secondly, northern cities experience colder winters, necessitating prolonged central heating, which significantly increases the demand for thermal and electrical energy [37], thereby contributing to higher per capita CO_2 emissions in the northern regions. Conversely, the southern regions have witnessed significant advancements in innovation and economic growth, transforming and upgrading their industrial structure. This has resulted in the tertiary industry becoming a dominant economic driver with a lower contribution to city CO_2 emissions compared to the secondary industry. Consequently, per capita CO_2 emissions in the southern region are generally lower than those in the northern region.

CO_2 Emissions Per Capita in Provincial Capitals and Independent-Plan Cities is Generally Higher Than that in Their Neighboring Cities

Per capita CO_2 emissions in provincial capitals and independent-plan cities are generally higher than those in surrounding cities (as shown in Fig. 3). In China's development strategy, provinces and autonomous regions prioritize the enhancement of the construction level of provincial capitals and independent-plan cities, exacerbating the disparity in comprehensive socio-economic development between these core cities and their surroundings. Residents in these areas typically enjoy higher living standards and possess more energy-consuming products, such as cars, which increases energy demand [38]. This increase in demand also drives the expansion of transportation infrastructure and other public facilities, the integrated development of industries, and contributes to elevated CO_2 emissions in surrounding cities [39]. Moreover, buildings in these cities, especially office towers and shopping malls, consume significantly more energy in operation and maintenance compared to a significantly higher overall energy demand in provincial capitals and independent-plan cities, leading to per capita CO_2 emissions notably higher than the average level in surrounding areas.

Spatiotemporal Dynamics of City Per Capita CO_2 Emissions

The spatial aggregation of per capita CO_2 emissions in Chinese cities is pronounced. Calculating the global Moran's I index for per capita CO_2 emissions at the prefecture level across the years 2000, 2005, 2010, 2015, and 2020 resulted in positive values, with respective scores of 0.511, 0.553, 0.617, 0.520, and 0.693. Each score passed the 1% significance test. This demonstrates a significant spatial clustering of per capita CO_2 emissions at the city scale, indicating that cities with higher and

lower per capita CO_2 emissions tend to be spatially proximate to one another.

LISA Time Path of Per Capita CO_2 Emissions

The relative length of the LISA time path is longer in the northern regions compared to the southern regions (Fig. 4), suggesting that the local spatial structure of per capita CO_2 emissions in northern cities is more dynamic, whereas the southern regions are relatively stable.

Overall, cities with a relative length of the LISA time path greater than 1 are predominantly concentrated in the North China Plain and Northwest, as well as in some other regions, especially in resource-based cities within these areas. From 2000 to 2020, among 336 city units studied, the average relative length of the LISA time path was 1, with 108 cities exceeding this threshold, accounting for approximately 32%. These cities are mainly resource-based and include some economically developed areas. Conversely, cities with a relative LISA time path length of less than 1 are predominantly located in southern cities. From 2000 to 2010, 38 cities exceeded this threshold, increasing to 99 cities, indicating a rise from 11% to 29%. The reason for this phenomenon is that resource-based cities are highly sensitive to policy and market influences, with fluctuations in city CO_2 emissions growth and local spatial dependence changes being strong.

Due to the presence of many resource-based cities in the north that are dominated by high-carbon-emitting secondary industries, exhibit pronounced resource reserves and exploit economic development. Since 2000, the development of resource-based industries has been highly sensitive to resource-related policies, the cyclical nature of government control policies, and market demand for these industries [40]. Furthermore, in some cities, prolonged resource exploitation has led to depletion, necessitating a shift towards industrial upgrades and transformations, thereby contributing to gradual reductions in per capita CO_2 emissions.

LISA Spatiotemporal Transition

The study utilizes LISA Spatiotemporal Transition to analyze the evolution of local spatial association types in city CO_2 emissions (Fig. 5).

(1) Per capita CO_2 emissions in Chinese cities show a more stable spatial structure.

Table 1 shows that from 2000 to 2020, per capita CO_2 emissions in Chinese cities exhibit a strong spatiotemporal cohesion probability (SC) of 85%, with a spatiotemporal transition probability (SF) of 15%. Type0 predominates at 77.1%, reflecting the strong path-locking characteristics of spatiotemporal transitions in prefecture-level units. The probabilities of the four spatiotemporal transition types are Type0 (0.771)>Type1 (0.095)>Type3 (0.074)>Type2 (0.060), indicating that the dominant position has not occurred in the transfer of spatial correlation forms, and the transfer of spatial correlation types exhibits varying degrees of transition inertia.

For Type0, the most stable transition probability of spatial correlation is LL→LL (0.861), and the transition probability from low-carbon cities to low-carbon spatial correlation is the highest, indicating that most cities can drive economic prosperity through green and low-carbon systems in the development process, and cities with low per capita CO_2 emission values have clustered development. Furthermore, a small portion of high-value per capita CO_2 emissions from HH have broken the path lock of cities, and CO_2 emissions from these cities or adjacent cities have shown a trend towards low-carbon development.

(2) A limited number of cities in China display characteristics of spatiotemporal transition in per capita CO_2 emissions.

From the perspective of transition types, Type1 (0.095)>Type3 (0.074)>Type2 (0.060), with the highest spatial transition probability towards LL, indicating a gradual shift in some Chinese cities towards low-carbon emission patterns. Type1 is the primary transition type, suggesting that cities themselves are more active in spatiotemporal transitions, whereas the neighboring areas are relatively stable. For Type1, the highest spatial association transition probability is HL→LL (0.685), indicating a significant probability of high CO_2 emission cities transitioning to become low CO_2 emission cities. This shift may be achieved through enhanced energy efficiency and a shift in energy structure, as observed in cities such as Shenzhen, Wuhan, and Hangzhou, which have reduced their per capita CO_2 emissions due to population and industrial agglomeration effects, leading to improved energy efficiency. Similarly, cities such as Lanzhou and Panzhihua have achieved reductions through strategic shifts in energy utilization and fostering low-carbon industrial practices. In Type2, the highest spatial transition probability is LH→LL (0.320), indicating a reduction of per capita CO_2 emissions in certain areas due to the mitigating effects from neighboring areas. Technological innovations can notably reduce the CO_2 emission intensity of a region, exerting a negative spillover effect on the CO_2 emission intensity of adjacent areas, which in turn leads to a substantial decrease in CO_2 emissions in those neighboring areas. Cities such as Jinhua, Zhoushan, and Nantong have improved energy efficiency and reduced per capita CO_2 emissions due to the influence of low-carbon technologies from neighboring low-carbon cities [41]. In Type3, the highest spatial transition probability is HH→LL (0.182), primarily observed in provincial capitals such as Harbin, Changchun, Jilin, Shanghai, and Ningbo. This transition may be attributed to the influence of economic shifts towards low-carbon industries, leading to a gradual decrease in per capita CO_2 emissions.

Table 1. Local Moran's I Transfer probability matrices and spatiotemporal variability.

2000/2020	HH	LH	LL	HL	Type	n	Percent	SF	SC
HH	0.677	0.107	0.182	0.032	Type0	259	0.771	0.150	0.850
LH	0.240	0.440	0.320	0.000	Type1	32	0.095		
LL	0.062	0.062	0.861	0.013	Type2	20	0.060		
HL	0.315	0.000	0.685	0.000	Type3	25	0.074		

Analysis of Factors Influencing City-Scale CO_2 Emissions

In this study, per capita CO_2 emissions (*PCCE*) are the dependent variable. Per capita GDP (*PCGDP*) and its square term, urbanization rate (*URB*), population size (*POP*), the share of value added by secondary industry in GDP (*SIP*), the share of value added by tertiary industry in GDP (*TIP*), the share of fixed investment assets in GDP (*INV*), and the share of total imports and exports in GDP (*IEP*) are taken as independent variables. The STIRPAT extended model with panel data is utilized for regression analysis, with results presented in Table 2.

Results of Regression Estimation

The results of the study are shown in Table 2. Where all five models employed fixed-effects estimators as deemed appropriate by the Hausmann test.

(1) An inverted U-shaped relationship between economic growth and environmental pollution in China at the city scale

Models 1–5 all include the variable "per capita GDP" and its squared term to investigate the Environmental Kuznets Curve (EKC) hypothesis. Results indicate a positive correlation between per capita GDP and CO_2 emissions, while the squared terms show a negative correlation, suggesting an inverted U-shaped relationship between economic growth and CO_2 emissions. Overall, economic growth influences CO_2 emissions through three main effects: scale, structure, and technology. With the growth of the economic scale, the demand for energy increases, leading to an increase in CO_2 emissions. Simultaneously, economic growth also brings about changes in economic structure, transitioning from a high-pollution industrial economy to a cleaner service-oriented and technology-driven economy, resulting in a decrease in CO_2 emissions. Moreover, technological advancements driven by economic growth enable more effective strategies to mitigate CO_2 emissions.

(2) Population size, fixed investment assets as a share of GDP, and per capita CO_2 emissions show a positive correlation

Population size positively impacts CO_2 emissions, indicating that population growth increases energy consumption and per capita CO_2 emissions. The proportion of fixed investment assets is also positively correlated with per capita CO_2 emissions. Historically, fixed asset investment in Chinese cities has concentrated on high-energy-consuming and high-polluting industries [42]. This study reveals that fixed-asset investment contributes to the expansion of energy-intensive sectors like transportation, construction, and manufacturing industries, thereby escalating CO_2 emissions. Conversely, the negative correlation between the urbanization rates and per capita CO_2 emissions indicates that urbanization promotes economic growth and energy efficiency through the agglomeration effect and economies of scale, consequently reducing per capita CO_2 emissions.

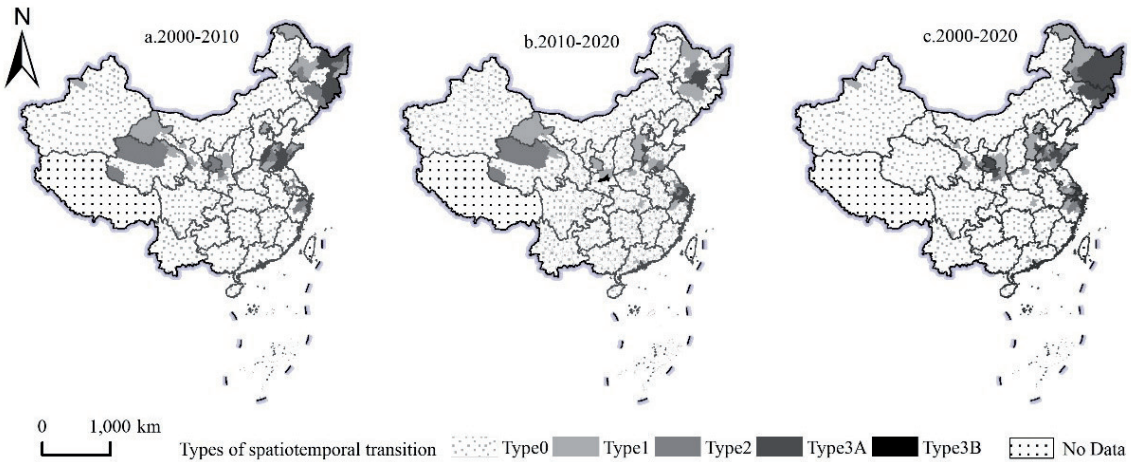

Fig. 5. Distribution map of spatiotemporal transition types in China.

Table 2. Regression results.

	model1	model2	model3	model4	model5
lnpcgdp	1.042***	1.173***	0.606***	0.582***	0.583***
	(0.0962)	(0.0937)	(0.108)	(0.107)	(0.108)
lnpcgdp_s	-0.0427***	-0.0339***	-0.0143**	-0.0143**	-0.0144**
	(0.00483)	(0.00473)	(0.00508)	(0.00507)	(0.00507)
URB		-0.384***	-0.289***	-0.269***	-0.269***
		(0.0703)	(0.0697)	(0.0698)	(0.0698)
lnpop		0.394***	0.204***	0.180***	0.181***
		(0.0274)	(0.0316)	(0.0321)	(0.0322)
SIP			0.347***	0.373***	0.373***
			(0.0823)	(0.0824)	(0.0824)
TIP			-0.439***	-0.391***	-0.392***
			(0.0820)	(0.0827)	(0.0827)
INV				0.0304***	0.0304***
				(0.00744)	(0.00744)
IEP					0.000601
					(0.00307)
lnyear	37.74***	-16.70**	27.30***	30.47***	30.41***
	(2.778)	(5.309)	(6.252)	(6.288)	(6.297)
_cons	-291.3***	114.8**	-213.3***	-236.9***	-236.4***
	(21.14)	(39.92)	(46.87)	(47.14)	(47.21)
N	4544	4544	4544	4544	4544
R^2	0.509	0.538	0.556	0.557	0.557
Hausman test	60.61***	144.80***	60.80***	87.15***	62.19***
AIC	-3929.7	-4203.6	-4375.4	-4391.2	-4389.3
BIC	-3904.1	-4165.1	-4324.0	-4333.4	-4325.1

Note: * p<0.05, ** p<0.01, *** p<0.001.

(3) Industrial structure is closely related to per capita CO_2 emissions

The regression results show that the proportion of added value from secondary industry in GDP is positively correlated with per capita CO_2 emissions, whereas the proportion of added value from tertiary industry in GDP is negatively correlated with per capita CO_2 emissions. China's manufacturing sector predominantly occupies the middle and lower ends of the value chain, characterized by a high concentration of energy-intensive industries like iron and steel, non-ferrous metals, building materials, petrochemicals, and chemicals, which tend to increase per capita CO_2 emissions as their share in the economic structure grows.

(4) The relationship between the intensity of import and export trade on CO_2 emissions is not clear yet.

Two hypotheses address the impact of foreign trade on CO_2 emissions: the "Pollution Haven Hypothesis" (PHV) and the "Pollution Halo Hypothesis" (PHL). The PHV theorizes that pollution-intensive industries tend to be established in countries with laxer environmental regulations due to technology spillover effects. Developing countries may gain comparative advantages in high-pollution and high-energy-consuming industries due to weaker environmental standards, making them destinations for the relocation of pollution industries from developing nations. In contrast, the PHL suggests that multinational enterprises can improve the energy efficiency of their host countries through technology spillover, thereby helping to reduce CO_2 emissions. Our regression shows that the ratio of total import and export to GDP is positively associated with CO_2 emissions, but this relationship does not pass the significance test,

which may be due to the complexity of the relationship between the degree of import and export trade on CO_2 emissions, making it challenging to draw consistent conclusions.

Discussion

(1) There are significant regional differences in per capita CO_2 emissions in Chinese.

Our results show that there are significant spatial differences in per capita CO_2 emissions in Chinese cities, showing that the per capita CO_2 emissions of northern cities are greater than those of southern cities, which is consistent with previous studies [43], and that the per capita CO_2 emissions of provincial capitals and independent-plan cities are generally higher than those of surrounding cities.

(2) The environmental Kuznets curve still refers to the Chinese city scale.

Our empirical results show that the inverted U-shaped relationship between economic growth and environmental pollution still exists at the prefecture level in China, aligning with previous studies [8]. Prior studies have found an inverted U-shaped relationship between economic growth and CO_2 emissions at the provincial level, and recent work has extended this examination to the prefecture level. Specifically, research has found that there is an inverted U-shaped relationship between economic growth and CO_2 emissions in consecutive single years from 1992 to 2013 [9]. Our empirical analysis extends this conclusion, validating its relevance to 2020.

(3) Population size is positively correlated with per capita CO_2 emissions in cities.

Our research findings indicate that population growth promotes per capita CO_2 growth, but in 2022, China experienced its first decline in total population, prompting the government to propose policy measures aimed at increasing fertility rates. While population growth typically correlates with higher CO_2 emissions, promoting a green lifestyle remains a crucial strategy for mitigating this impact, particularly in the context of rising birth rates. Examples of such lifestyle changes include implementing waste sorting, avoiding extreme air conditioning temperatures, adopting eco-friendly modes of transportation, and so on [44].

(4) Our findings reveal that the proportion of value added by secondary industry in GDP is positively correlated with per capita CO_2 emission, whereas the proportion of value added by tertiary industry in GDP is negatively correlated with per capita CO_2 emissions.

This is consistent with the findings of Zhao et al. [45], suggesting that China could reduce its CO_2 emission intensity by optimizing its industrial structure. It is noteworthy that the total imports and exports are not correlated with per capita CO_2 emissions in our regression results, whereas Haug and Ucal [46] showed that an increase in the total imports and exports as a share of GDP increases per capita CO_2 emissions, and at the same time, there are also studies that find that the total imports and exports as a share of GDP mitigate per capita CO_2 emissions [47]. The advancement of urbanization will bring about population and industrial agglomeration, promote technological progress, improve total factor productivity, and increase income levels. This is precisely because agglomeration brings facility utilization efficiency and reduces per capita CO_2 emissions that our findings are consistent with the study by Wang et al. [48].

Limitations and Prospects

The research in this paper still has some uncertainties and limitations. First, based on methodologies proposed by Ou et al. [12] and Chen et al. [13], we developed a set of methods for downscaling estimation of CO_2 emissions, but the accuracy of this method can be further improved. On the one hand, the abnormally high nighttime light brightness in resource-based cities may overestimate their CO_2 emissions. On the other hand, further discussion is needed to determine the per capita CO_2 emissions in the dark areas. Meanwhile, although this paper corrects the landscan population dataset based on the Chinese census data and the national 1% population sample survey data, there is still some discrepancy in the population number on a small scale, and the correction of the population raster data can be considered in the future using a finer scale. In terms of influencing factors, due to the limitation of data acquisition, this paper did not consider the influence of factors such as energy structure and technological progress on per capita CO_2 emissions. If there are relevant data released in the future, such factors should be included in the analysis.

Conclusions

China implements a top-down management system, which decomposes the tasks of CO_2 emissions at different administrative levels. Estimating CO_2 emissions and their influencing factors at the city scale is of great significance for each local government in order to carry out the reduction of per capita CO_2 emissions. Therefore, this paper estimates the per capita CO_2 emissions at the city scale based on the population raster data, nighttime light data, and energy consumption data; we applies ESTDA method to analyze the spatial and temporal pattern of per capita CO_2 emissions in Chinese cities from 2000 to 2020; and investigates the influencing factors based on the STIRPAT extended model using panel data regression. The main conclusions are as follows:

(1) In terms of overall distribution patterns, per capita CO_2 emissions are characterized by uneven spatial distribution in Chinese cities.

Per capita CO_2 emissions in northern cities are generally higher than those in southern cities, which may be due to the fact that northern cities are richer in fossil energy resources such as coal, oil, and natural gas; furthermore, their development is highly reliant on carbon-intensive industries, and their total population is relatively small, which results in higher per capita CO_2 emissions. Some provincial capitals and cities with separate plans have higher per capita CO_2 emissions than their neighboring cities, mainly due to the higher living standards of their residents and their higher demand for energy in daily life.

(2) From 2000 to 2020, the per capita CO_2 emissions of Chinese cities show significant spatial agglomeration characteristics in terms of spatiotemporal dynamics. The overall stability is evidenced by an 85% spatiotemporal cohesion rate during this period. Among the categories, Type0 category has the highest proportion of spatiotemporal transitions, while the majority remained unchanged in their correlation patterns. From the viewpoint of its subtypes, the LL type is the most stable, indicating the continuity of development. The probability of the transformation of the HH type is 30.9%, suggesting only some of the cities in high carbon-emission agglomerations underwent transformation and development. Local changes are reflected in the fact that from 2000 to 2020, the rate of spatiotemporal transitions is 15%, and from the subtypes of the three types of spatiotemporal transitions, Type1 (0.095)>Type3 (0.074)>Type2 (0.060), all of which indicate that the development trend of low carbon transformation has emerged in some of China's resource-based cities.

(3) There is an inverted U-shaped relationship between per capita GDP and per capita CO_2 emissions, with positive correlations between population size, the proportion of value added by the secondary industry to GDP, and the proportion of fixed investment assets to GDP and per capita CO_2 emissions. There are negative correlations between the level of urbanization, the proportion of value added by the tertiary industry to GDP, and per capita CO_2 emissions.

Acknowledgments

This research was funded by the Chongqing Social Science Planning Project (Grant No. 2022BS080), High-level Talent Research Startup Project of Chongqing Technology and Business University (Grant No. 2356028), the Youth Fund Project of Humanities and Social Science Research plan of the Ministry of Education (20YJC790091), the project of Scientific Research Foundation of Chongqing Technology and Business University (Grant No.1956027).

Conflict of Interest

The authors declare no conflict of interest.

References

1. IPCC Climate Change 2021: The Physical Science Basis. Contribution of Working Group I to the Sixth Assessment Report of the Intergovernmental Panel on Climate Change. Cambridge University Press, Cambridge, United Kingdom and New York, NY, USA. **2021**.
2. IEA CO_2 Emissions in 2022. IEA, Paris. **2023**.
3. WEI W., ZHANG X., CAO X., ZHOU L., XIE B., ZHOU J., LI C. Spatiotemporal dynamics of energy-related CO_2 emissions in China based on nighttime imagery and land use data. Ecological Indicators. **131**, 108132, **2021**.
4. ZHOU K., YANG J., YANG T., DING T. Spatial and temporal evolution characteristics and spillover effects of China's regional carbon emissions. Journal of Environmental Management. **325**, 116423, **2023**.
5. LEE C.C., ZHAO Y.N. Heterogeneity analysis of factors influencing CO_2 emissions: the role of human capital, urbanization, and FDI. Renewable and Sustainable Energy Reviews. **185**, 113644, **2023**.
6. LIU H., GOU P., XIONG J. Vital triangle: A new concept to evaluate urban vitality. Computers, Environment and Urban Systems. **98**, 101886, **2022**.
7. GHOSH T., ELVIDGE C.D., SUTTON P.C., BAUGH K.E., ZISKIN D., TUTTLE B.T. Creating a Global Grid of Distributed Fossil Fuel CO_2 Emissions from Nighttime Satellite Imagery. Energies. **3** (12), 1895, **2010**.
8. WANG Z.Y., YE X.Y. Re-examining environmental Kuznets curve for China's city-level carbon dioxide (CO_2) emissions. Spatial Statistics. **21**, 377, **2017**.
9. WANG S., LIU X. China's city-level energy-related CO_2 emissions: Spatiotemporal patterns and driving forces. Applied Energy. **200**, 204, **2017**.
10. CHEN Z., YU B., YANG C., ZHOU Y., YAO S., QIAN X., WANG C., WU B., WU J. An extended time series (2000–2018) of global NPP-VIIRS-like nighttime light data from a cross-sensor calibration. Earth System Science Data. **13** (3), 889, **2021**.
11. CHEN J., GAO M., CHENG S., HOU W., SONG M., LIU X., LIU Y., SHAN Y. County-level CO_2 emissions and sequestration in China during 1997–2017. Scientific data. **7** (1), 391, **2020**.
12. OU J., LIU X., LI X., LI M., LI W. Evaluation of NPP-VIIRS Nighttime Light Data for Mapping Global Fossil Fuel Combustion CO_2 Emissions: A Comparison with DMSP-OLS Nighttime Light Data. PLoS One. **10** (9), e0138310, **2015**.
13. CHEN H., ZHANG X., WU R., CAI T. Revisiting the environmental Kuznets curve for city-level CO_2 emissions: based on corrected NPP-VIIRS nighttime light data in China. Journal of Cleaner Production. **268**, 121575, **2020**.
14. GROSSMAN G.M., KRUEGER A.B. Environmental Impacts of a North American Free Trade Agreement. National Bureau of Economic Research Working Paper Series. **3914**, **1991**.
15. HE P., YA Q., CHENGFENG L., YUAN Y., XIAO C. Nexus between Environmental Tax, Economic Growth, Energy Consumption, and Carbon Dioxide Emissions: Evidence from China, Finland, and Malaysia Based on a Panel-ARDL Approach. Emerging Markets Finance and

Trade. **57** (3), 698, **2021**.
16. PATA U.K., CAGLAR A.E. Investigating the EKC hypothesis with renewable energy consumption, human capital, globalization and trade openness for China: evidence from augmented ARDL approach with a structural break. Energy. **216**, 119220, **2021**.
17. WU Y., SHI K., CHEN Z., LIU S., CHANG Z. Developing Improved Time-Series DMSP-OLS-Like Data (1992-2013;2019) in China by Integrating DMSP-OLS and SNPP-VIIRS. IEEE Transactions on Geoscience and Remote Sensing. **60**, 1, **2022**.
18. HUANG J., ZHONG P., ZHANG J., ZHANG L. Spatial-temporal differentiation and driving factors of ecological resilience in the Yellow River Basin, China. Ecological Indicators. **154**, 110763, **2023**.
19. CHENG Y., WANG Z., YE X., WEI Y. Spatiotemporal dynamics of carbon intensity from energy consumption in China. Journal of Geographical Sciences. **24**, **2014**.
20. ELVIDGE C., BAUGH K., SUTTON P., BHADURI B., TUTTLE B., TILOTTAMA G., ZISKIN D., ERWIN E. Who's in the Dark—Satellite Based Estimates of Electrification Rates. In book Urban Remote Sensing: Monitoring, Synthesis and Modeling in the Urban Environment. Editor Xiaojun Yang, Wiley-Blackwell, Chichester, UK. **2011**.
21. REY S.J., JANIKAS M.V. STARS: Space–Time Analysis of Regional Systems. Geographical Analysis. **38** (1), 67, **2006**.
22. REY S.J., YE X. Comparative Spatial Dynamics of Regional Systems. Springer Berlin Heidelberg, Berlin, Heidelberg. **2010**.
23. ANSELIN L. The Moran scatterplot as an ESDA tool to assess local instability in spatial association. Spatial Analytical Perspectives on GIS, Routledge, pp.111-126. **2019**.
24. YE X., REY S. A framework for exploratory space-time analysis of economic data. The Annals of Regional Science. **50** (1), 315, **2013**.
25. REY S.J., MURRAY A.T., ANSELIN L. Visualizing regional income distribution dynamics. Letters in Spatial and Resource Sciences. **4** (1), 81, **2011**.
26. YORK R., ROSA E.A., DIETZ T. STIRPAT, IPAT and ImPACT: analytic tools for unpacking the driving forces of environmental impacts. Ecological economics. **46** (3), 351, **2003**.
27. ASLAM B., HU J., SHAHAB S., AHMAD A., SALEEM M., SHAH S.S.A., JAVED M.S., ASLAM M.K., HUSSAIN S., HASSAN M. The nexus of industrialization, GDP per capita and CO_2 emission in China. Environmental Technology & Innovation. **23**, 101674, **2021**.
28. BALSALOBRE-LORENTE D., DRIHA O.M., HALKOS G., MISHRA S. Influence of growth and urbanization on CO_2 emissions: The moderating effect of foreign direct investment on energy use in BRICS. Sustainable Development. **30** (1), 227, **2022**.
29. XU L., CUI S., TANG J., YAN X., HUANG W., LV H. Investigating the comparative roles of multi-source factors influencing urban residents' transportation greenhouse gas emissions. Science of The Total Environment. **644**, 1336, **2018**.
30. SALMAN M., LONG X., DAUDA L., MENSAH C.N., MUHAMMAD S. Different impacts of export and import on carbon emissions across 7 ASEAN countries: A panel quantile regression approach. Science of the Total Environment. **686**, 1019, **2019**.
31. HASHMI R., ALAM K. Dynamic relationship among environmental regulation, innovation, CO_2 emissions, population, and economic growth in OECD countries: A panel investigation. Journal of Cleaner Production. **231**, 1100, **2019**.
32. BEN JEBLI M., FARHANI S., GUESMI K. Renewable energy, CO_2 emissions and value added: Empirical evidence from countries with different income levels. Structural Change and Economic Dynamics. **53**, 402, **2020**.
33. WEN H.X., CHEN Z., YANG Q., LIU J.Y., NIE P.Y. Driving forces and mitigating strategies of CO_2 emissions in China: A decomposition analysis based on 38 industrial sub-sectors. Energy. **245**, 123262, **2022**.
34. SU W., LIU Y., WANG S., ZHAO Y., SU Y., LI S. Regional inequality, spatial spillover effects, and the factors influencing city-level energy-related carbon emissions in China. Journal of Geographical Sciences. **28**, 495, **2018**.
35. CHEN Y., WANG Z., ZHONG Z. CO_2 emissions, economic growth, renewable and non-renewable energy production and foreign trade in China. Renewable Energy. **131**, 208, **2019**.
36. FAN J.J., WANG J.L., QIU J.X., LI N. Stage effects of energy consumption and carbon emissions in the process of urbanization: Evidence from 30 provinces in China. Energy. **276**, **2023**.
37. CUI C., SHAN Y., LIU J., YU X., WANG H., WANG Z. CO_2 emissions and their spatial patterns of Xinjiang cities in China. Applied Energy. **252**, **2019**.
38. ZHONG Y., LIN A., XIAO C., ZHOU Z. Research on the spatio-temporal dynamic evolution characteristics and influencing factors of electrical power consumption in three urban agglomerations of Yangtze River Economic Belt, China based on DMSP/OLS night light data. Remote Sensing. **13** (6), 1150, **2021**.
39. SU L. Temporal-Spatial Evolution Characteristics and Influencing Factors of Urban Carbon Emissions in China. Polish. **32** (3), 2309, **2023**.
40. LI Q., ZENG F.E., LIU S., YANG M., XU F. The effects of China's sustainable development policy for resource-based cities on local industrial transformation. Resources Policy. **71**, 101940, **2021**.
41. FENG M., LAN L., CHEN C., ZHU Y. Spatial Effect Research on the Impact of Technological Innovation on Carbon Dioxide Emission Intensity. Polish Journal of Environmental Studies. **31** (6), 5675, **2022**.
42. SHUAI C., CHEN X., WU Y., TAN Y., ZHANG Y., SHEN L. Identifying the key impact factors of carbon emission in China: Results from a largely expanded pool of potential impact factors. Journal of Cleaner Production. **175**, 612, **2018**.
43. ZHANG H., LI Y., TONG J. Spatiotemporal differences in and influencing effects of per-capita carbon emissions in China based on population-related factors. Scientific Reports. **13** (1), 20141, **2023**.
44. ZHANG J., ZHENG T. Can dual pilot policy of innovative city and low carbon city promote green lifestyle transformation of residents. Journal of Cleaner Production. **405**, 136711, **2023**.
45. ZHAO J., JIANG Q., DONG X., DONG K., JIANG H. How does industrial structure adjustment reduce CO_2 emissions? Spatial and mediation effects analysis for China. Energy Economics. **105**, 105704, **2022**.
46. HAUG A.A., UCAL M. The role of trade and FDI for CO_2 emissions in Turkey: Nonlinear relationships. Energy Economics. **81**, 297, **2019**.
47. DING T., NING Y., ZHANG Y. The contribution of

China's bilateral trade to global carbon emissions in the context of globalization. Structural Change and Economic Dynamics. **46**, 78, **2018**.

48. WANG W.Z., LIU L.C., LIAO H., WEI Y.-M. Impacts of urbanization on carbon emissions: An empirical analysis from OECD countries. Energy Policy. **151**, 112171, **2021**.